Micro Turbojet Engine Design Project Report

Seitzman AE4453 Fall 2025

Daniel Elliott | Nishchal Anekere

11/18/2025

INTRODUCTION

The objective of this project is to perform a preliminary design of the components of a micro turbojet intended for use in a large UAV. This design is based on a preliminary cycle design study which was carried out with the target of developing an engine design which could produce 4.3 kN of thrust while the UAV cruises at M = 0.8. At this operating condition, the study prescribed ambient conditions of T = 249.0 K, P = 45.1 kPa, and h = ~21 kft. It also identified the need for the engine to operate on a single spool, have a compressor stagnation pressure ratio of 10.9 including the IGV and OGV components, avoid the need for bleed-air cooling by constraining turbine inlet temperature (T_{o4}) to 1680K, and function with an air mass flow rate of 5.02 kg/s and a fixed area nozzle.

This preliminary design is intended to provide a more accurate estimate of maximum thrust under the given operating conditions compared to the preliminary cycle design study. It also provides thrust estimations for an alternate cruise condition with conditions of h = 41 kft, T = 216.7 K, P = 17.9 kPa, and M = 0.92, with throttling varying T_{o4} from 1500-1700 K. The thrust estimation that this design study provides at the given operating conditions will serve to confirm the validity of the results and initial conditions and constraints of the cycle design study.

To accomplish this, individual components were designed, analyzed, and optimized using an iterative gradient-based optimization loop. Component-level efficiencies were each optimized in the direction of maximum thrust as described below, and overall engine thrust was also maximized. Various constraints were imposed on each component to ensure the end result was both realistic and practical.

APPROACH

Engine (high level)

The solver, written in MATLAB, is constructed from a series of nested fmincon optimization functions, starting with a top-level engine optimization function. This function defines all givens, constraints, and properties that govern the performance of the engine and its components. Its fmincon optimizer employs two design variables – the pressure ratio of the first compressor stage, and the work ratio (ie, the proportion of total work performed) of the first turbine stage. Two additional design variables are selected by the user – the number of compressor stages and the number of turbine stages, since these variables are discrete integers which do not mesh well with fmincon's gradient-based solution strategy. The objective of this fmincon optimizer is to maximize the thrust produced by the engine – accomplished by setting -1 * thrust as the value returned by the objective function. The only nonlinear constraint employed at this level is an equality constraint to ensure that the compressor's total pressure ratio is equal to the required pressure ratio – this is verified at a lower component level but was included here for redundancy.

Within the engine optimization function, the compressor is optimized first, followed by the combustor and the turbine. Simple, non-optimizing computation functions then analyze the diffuser and the nozzle using inputs from those three primary components, which enables the calculation of thrust, which is passed back to the engine-level optimizer. Component-level constraints are employed in their relevant optimizers and will be explained in further detail below. A simplified schematic illustrating the primary relationships between components is given below for reference.

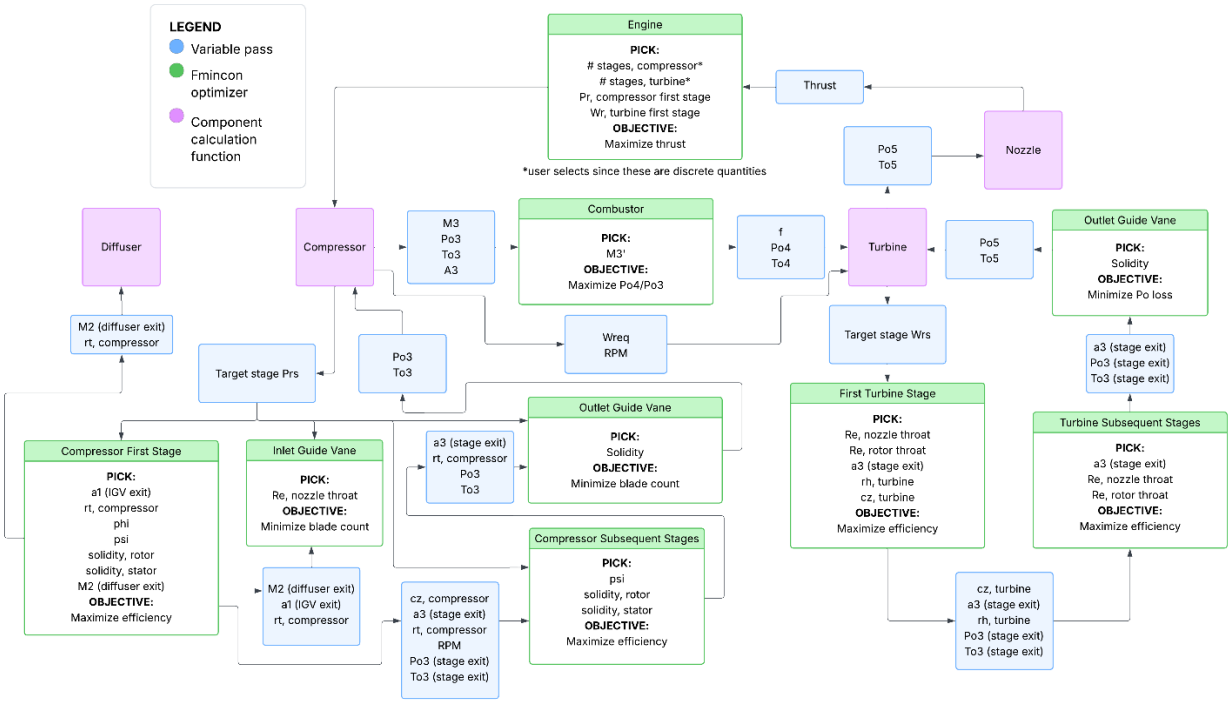

Ultimately, seven compressor stages and one turbine stage were used to meet the design requirements. Fewer than seven compressor stages resulted in reduced efficiency, which increased the turbine work requirement and decreased thrust. With seven compressor stages, one turbine stage was able to meet the work requirement, minimizing Po loss going into the nozzle and producing higher thrust. Practically, designing, manufacturing, and maintaining an additional turbine stage is more challenging and expensive than doing so for a compressor stage on account of the turbine's much more extreme operating conditions, so this trade was worthwhile.

To avoid repeating commonly used equations needed for calculations in multiple components, equations used generally across the code are listed below.

EQUATIONS USED - GENERAL	
$\boldsymbol{h = r_t - r_h}$	Used to obtain blade heights
$(U = r\Omega)$	Used to obtain blade velocities

$\frac{p}{p_t} = \left(1 + \frac{\gamma - 1}{2} M^2\right)^{\frac{-\gamma}{\gamma - 1}}$	Used to obtain static pressures
$\frac{T}{T_t} = \left(1 + \frac{\gamma - 1}{2} M^2\right)^{-1}$	Used to obtain static temperature
$\rho = \frac{P}{RT}$	Used to obtain densities
$c_{\theta_i} = c_i \sin \alpha_i = c_{z_i} \tan \alpha_i$	Used to obtain velocities, angles in casing frame
$w_{\theta_i} = w_i \sin \beta_i = w_{z_i} \tan \beta_i$	Used to obtain velocities, angles in rotor frame
$M = \frac{u}{\sqrt{\gamma RT}}$	Used to obtain Mach numbers, abs and rel
$\dot{m} = \rho c_z \pi \left(r_t^2 - r_h^2\right)$	Used to obtain blade radii
$r_m^2 = \sqrt{\frac{r_t^2 + r_h^2}{2}}$	Used to obtain pitchline radii
$\sigma = \frac{b}{s}$	Used to obtain b or s from solidity
$s = \frac{2\pi r}{n_{blades}}$	Used to calculate blade counts
$AR_{blade} = \frac{h}{b}$	Used to calculate blade aspect ratios
$\nu = \frac{\mu}{\rho}$	Used to calculate kinematic viscosity from dynamic
$R = \frac{\overline{R}}{MW}$	Used to calculate specific gas constant
$C_p = \frac{R\gamma}{\gamma - 1}$	Used to calculate specific heat
$\mu = \mu(T_{ref}) * \left(\frac{T}{T_{ref}}\right)^{0.7}$	Used to scale viscosity with temperature
$AN^2 = \pi({r_{tr}}^2 - {r_{hr}}^2) * N^2$	Used to obtain AN^2 parameter
$\sigma_{cent} = \Omega^2 (r_t - r_h) * \left[\left(\frac{r_t + 2r_h}{6}\right) + \frac{A_t}{A_h}\left(\frac{2r_t + r_h}{6}\right)\right]$	Used to calculate centrifugal blade stress
$\sigma_{bend} = \left(\frac{p_1 + p_2}{2}\right) * \frac{c_z}{U_{tip}} * \frac{\lvert\Delta h_{o1,3}\rvert}{c_p T_{o1}} * \frac{1}{2\sigma} * \left(\frac{r_{tip}}{t_{max}}\right)^2$	Used to calculate bending blade stress
$\dot{m} = \frac{A\, p_t}{\sqrt{T_t}} \sqrt{\frac{\gamma}{R}}\, M \left(1 + \frac{\gamma - 1}{2} M^2\right)^{-\frac{\gamma + 1}{2(\gamma - 1)}}$	General mass flow equation (used for off-design calculations and for nozzle throat/exit area)
$\eta_{st} = \frac{\mathrm{Pr}_{st}^{\gamma - 1/\gamma} - 1}{T_{o3}/T_{o1} - 1}$	Used to calculate compressor efficiencies (overall and stage)

$^{\circ}R = \frac{\Delta h_{rotor}}{\Delta h_{stage}}$	Used to calculate degree of reaction

Compressor (component level)

The compressor is comprised of an inlet guide vane (henceforth referred to as the IGV), seven individual stages, and an outlet guide vane (referred to as the OGV). First, the compressor calculates the necessary pressure ratio for each stage. It uses the first stage pressure ratio chosen at the engine level, the number of stages as dictated by the user, the required overall pressure ratio, and two assumed pressure ratios for the IGV and OGV to calculate what each stage's pressure ratio should be, assuming that the pressure ratios decrease linearly along the compressor's axis while all multiplying together to the required overall pressure ratio. Using assumed pressure ratios for the IGV and OGV allows the first compressor stage to pick important quantities without having to backtrack on its tip radius, inlet velocity, or inlet static properties later.

To begin, the first stage of the compressor is optimized by a unique fmincon function with more design variables than later stages. This optimizer first picks a1 (swirl angle at IGV exit/first stage inlet), rt (compressor tip radius), phi (flow coefficient), psi (stage loading coefficient), solidities for rotor and stator, and M2 (mach number at diffuser exit/IGV inlet, assuming constant cz across the IGV. Next, it calculates all rotor radii using mass flow continuity, cz, mdot, rt, and a1, then performs velocity triangle analysis using psi, phi, cz, and a1 to determine velocities and angles at each station throughout the stage. It assumes that a3 is offset from a1 by 2.5 degrees for this and all subsequent stages and constrains the selected a1 such that a3 of the final stage will be less than 44 degrees. Finally, it calculates diffusion factors and pressure ratios for each blade row using solidities, station Mach numbers, and flow angles. It also calculates stator radii using stagnation properties at station 2, mass flow continuity, cz, mdot, rt, and a2 before calculating blade dimensions and Reynolds numbers using tip/hub radii, static properties at stations 1 and 2, solidities, and the minimum allowable blade aspect ratio of 1.1, which was manually selected to give the longest blade chord (and highest Reynold's number) possible to make meeting that constraint easy. Solidities are also adjusted such that blade counts are whole. Next, it enforces an equality constraint to ensure the stage meets its target pressure ratio, while also enforcing the specified inequality constraints on M1rel, diffusion factors for rotor and stator, and blade Reynold's number for rotor and stator. Once the first stage has been optimized to maximize efficiency, it calculates metal angles, blade stresses, and work required before passing outlet stagnation properties, a3, rt, cz, and N (spool RPM as calculated from selected phi and resultant rotor rm) forward to the next stage and rt, a1, and M2 back to the inlet guide vane.

The second stage functions nearly identically to the first, just with fewer design variables since the first stage has picked them. It takes the thermodynamic and

component-level quantities from the first stage, then picks psi and stator/rotor solidities to hit the target stage pressure ratio supplied by the compressor while meeting the same constraints as described above for the first stage. Analysis methods are identical, and the optimizer functions under an identical assumption for the offset from a1 (received from the previous stage as its a3) to a3. When stage optimization (maximizing efficiency) is complete, the solver iterates to the next stage, and designs another stage in identical fashion, again using the outputs of the previous stage as the inputs to the next with the same constraints and objective in place. Metal angle, blade stress, and work calculations are all performed exactly as they were carried out for the first stage.

Once stage optimization is complete, the IGV and OGV are designed and optimized. The IGV is analyzed as a nozzle. Its optimizer picks nozzle throat Reynold's number as a design variable and seeks to minimize blade count (chosen to make manufacturing easier and keep cost/mass low). Since a1 was given as 0 degrees, a2 for the blade row and diffuser exit Mach were selected by the compressor, and stagnation pressure ratio was pre-selected to make pressure ratio assignments for each non-guide-vane stage easier, analysis is simple. It begins by performing velocity triangle analysis to determine swirl velocities and flow angles, then determines the hub radii and blade height using mass flow continuity and the compressor tip radius selected by the first stage. It then calculates optimum solidity for the blade row using the Zweifel criteria while ensuring that blade count is a whole number. Next, it calculates final blade dimensions and the stagnation pressure ratio across the blade row using Soderberg's correlation. Lastly, it enforces an equality constraint to ensure target pressure ratio is met.

The OGV is analyzed as a diffuser. Its optimizer picks solidity as a design variable and seeks to minimize blade count per the same rationale as the IGV. Inlet swirl angle a1 is given by the exit swirl angle a3 of the final compressor stage, and guide vane outlet angle a2 is required to be 0 degrees per the problem statement. Analysis is carried out in identical fashion to the stators of each compressor stage – velocity triangle analysis first using compressor cz, inlet stagnation properties, and flow angles, followed by mass flow continuity to obtain the hub radius given the compressor tip radius, then calculation of the diffusion factor and pressure ratio using chosen solidity (tuned to facilitate an integer blade count), flow velocities, and flow angles, and lastly, blade dimensions and Reynold's number. Relevant inequality constraints for M1rel, diffusion factor, and Re are imposed, as is an equality constraint verifying that the guide vane hits its prescribed pressure ratio.

With each stage of the compressor designed and optimized, the compressor function calculates the total work required to power it along with its polytropic efficiency. It then passes diffuser-relevant parameters selected by its first stage (namely, M2 and rt) to the diffuser, exit properties/parameters (Po3, To3, M3, A3) to the combustor, and spool

requirements (Wreq, RPM) to the turbine. Degree of reaction is also calculated for each individual compressor stage.

DESIGN PARAMETERS FOR OPTIMIZATION – FIRST STAGE	
a1	First stage inlet swirl angle/IGV exit swirl angle, casing reference frame
rt	Compressor tip radius
phi	Flow coefficient
psi	Stage loading coefficient
sigmaR	Rotor solidity
sigmaS	Stator solidity
M2	Mach at diffuser exit/IGV inlet

DESIGN PARAMETERS FOR OPTIMIZATION – SUBSEQUENT STAGES	
psi	Stage loading coefficient
sigmaR	Rotor solidity
sigmaS	Stator solidity

DESIGN PARAMETERS FOR OPTIMIZATION – INLET GUIDE VANE	
Reon	Reynold's number, nozzle throat

DESIGN PARAMETERS FOR OPTIMIZATION – OUTLET GUIDE VANE	
sigma	Blade row solidity

EQUATIONS USED - IGV	
$o/s \cong \cos\alpha_2$ (II.47a)	Used to calculate spacings
$Re_o\ (= c_2\, o / \nu_{throat})$	Used to calculate throat opening distances
$\delta \cong m\dfrac{\lvert\varphi\rvert}{\sigma}; m = \dfrac{1}{8}$	Used to calculate deviation at stator exit
(II.50) $\sigma_z \equiv b_z / s$	Used to calculate axial chord bz
(II.51a) $\sigma_z\psi_z = \left(\dfrac{c_{\theta_1}}{c_{\theta_2}} - 1\right)\sin(2\alpha_2)\left\{\dfrac{\gamma/2\,M_2^2}{\left(1+\dfrac{\gamma-1}{2}M_2^2\right)^{\gamma/(\gamma-1)} - 1}\right\}$	Used to calculate axial solidities
$\sigma = \sigma_z / \cos\xi$ (II.52)	Used to obtain non-axial solidities
(II.53a) $\xi \approx \alpha_{mean} = \tan^{-1}\left(c_{\theta mean}/c_z\right)$	Used to obtain eta angle

$c_{\theta_{mean}} = \frac{c_{\theta_1} + c_{\theta_2}}{2}$ (II.53b)	Used to obtain cthetamean
$\zeta = \left(\zeta^* C_j - 1\right)\left(\frac{10^5}{\mathrm{Re}_e}\right)^{1/4}$	Used to obtain energy loss coefficients
$\zeta^* = 1.04 + 0.06\left(\frac{\alpha_1 + \alpha_2}{100}\right)^2$	Used to obtain zeta* values
$C_{nozzle} = 0.993 + 0.021(b_z/h)$	Used to obtain C value
$\mathrm{Re}_e = \frac{\rho_2 c_2 D_h}{\mu_2}$	Used to obtain Reynold's numbers for energy loss calcs
$D_h = \frac{2sh\cos\alpha_2}{s\cos\alpha_2 + h}$	Used to obtain hydraulic diameter for Reynold's calcs
$\frac{p_{o1} - p_{o2}}{p_{o1}} = 1 - \left[\frac{1 - \frac{c_2^2}{2c_p T_{o1}}\frac{1}{1-\zeta}}{1 - \frac{c_2^2}{2c_p T_{o1}}}\right]^{\gamma/\gamma-1}$ (II.56)	Used to obtain Po losses across blade row
$\chi_2 = \alpha_2 + \delta_n$	Used to obtain chi2

EQUATIONS USED – COMPRESSOR STAGES AND OGV	
$D_{f,r} \approx 1 - \frac{\cos\beta_1}{\cos\beta_2} + \frac{1}{\sigma_r}\frac{\cos\beta_1}{2}(\tan\beta_2 - \tan\beta_1)$ $D_{f,s} \approx 1 - \frac{\cos\alpha_2}{\cos\alpha_3} + \frac{1}{\sigma_s}\frac{\cos\alpha_2}{2}(\tan\alpha_2 - \tan\alpha_3)$ (II.29)	Diffusion factors for both rotor and stator blade rows
$\frac{p_{o3}}{p_{o2}} = \left\{1 - \bar{\omega}_s\left[1 - \left(1 + \frac{\gamma-1}{2}M_2^2\right)^{\frac{\gamma}{1-\gamma}}\right]\right\}$ (II.32)	Pressure ratio for stator
$\frac{p_{o2}}{p_{o1}} = \left(\frac{1 + \frac{\gamma-1}{2}M_2^2}{1 + \frac{\gamma-1}{2}M_{2,rel}^2}\right)^{\frac{\gamma}{\gamma-1}}\left[1 - \varpi_r\left\{1 - \left(1 + \frac{\gamma-1}{2}M_{2,rel}^2\right)^{\frac{\gamma}{1-\gamma}}\right\}\right]\left(\frac{1 + \frac{\gamma-1}{2}M_{1,rel}^2}{1 + \frac{\gamma-1}{2}M_1^2}\right)^{\frac{\gamma}{\gamma-1}}$ (II.33)	Pressure ratio for rotor
$\eta_{st} = \frac{\mathrm{Pr}_{st}^{\gamma-1/\gamma} - 1}{U^2\psi/c_p T_{o1}}$	Used during optimization
$\delta \cong m\lvert\varphi\rvert/\sqrt{\sigma}$ *camber angle*	Carter's Rule for Deviation, used to assign metal angles after determining flow angles

(II.11) $i \equiv -(\beta_1 - \chi_1)$ (rotor) $i \equiv \alpha_2 - \chi_{2s}$ (stator)	Used in conjunction with the above for the same purpose
(II.12) $\delta \equiv -(\beta_2 - \chi_{2r})$ (rotor) $\delta \equiv \alpha_3 - \chi_3$ (stator)	^^
$\varpi \cong \left(\frac{\cos\alpha_1}{\cos\alpha_2}\right)^2 \frac{\sigma}{\cos\alpha_2}\left(0.012 + 0.0004e^{7.5\left[1-\frac{\cos\alpha_1}{\cos\alpha_2}+\frac{1}{\sigma}\frac{\cos\alpha_1}{2}\lvert\tan\alpha_1-\tan\alpha_2\rvert\right]}\right)$ pressure loss coeff correlates well with D_f	Absolute pressure loss parameter. Used by pressure ratio equations
$\psi = 1 + \phi(\tan\beta_2 - \tan\alpha_1)$ (II.22)	Used to obtain b2 given psi, phi, and a1
$\frac{c_z}{U} \equiv \phi$ (II.21)	Used to obtain U when necessary using cz and phi, no RPM
$\dot{W}/\dot{m} = \Delta(uc_\theta) = \Delta h_o$	Used to obtain work requirement
$\varphi = \chi_1 - \chi_2$ (II.8)	Used to obtain camber

CONSTRAINTS IMPOSED - COMPRESSOR	
$M_2 \leq 0.5$	Diffuser exit Mach number (since first compressor stage picks)
$D_f \leq 0.6$	Diffusion factor for rotors and stators
$Re_b > 2.5e5$	Blade chord Reynold's number
$M_{rel} \leq 0.79$	Mach number relative to each blade
$\frac{h}{b} = 1.1$	Blade aspect ratio – sitting at the lower end of the range was most favorable for Reynold's number constraint and did not impact losses
$\bar{\omega}_{eff} = \bar{\omega} * 2.3$	Pressure loss factor adjustment for secondary/tip losses
$R_{taper,diff} = 0.8$	Blade taper ratio for diffuser blade rows (all stages, OGV)
$R_{taper,IGV} = 0.5$	Blade taper ratio for IGV
$t_{diff} = 0.1 * b$	Maximum thickness for all stages/OGV – sitting at upper end of range was most favorable for blade stress
$1e5 \leq Re_o \leq 5e5$	Throat Reynold's number for IGV
$a_e = 0°$	Exit swirl from OGV
$a_{1,OGV} < 45°$	Exit swirl from compressor stages/inlet to OGV
$\lvert\psi_z\rvert = 0.8$	Zweifel parameter for IGV
$a_3 = a_1 + 2.5°$	Standard swirl offset for non-guide-vane stages

Combustor (component level)

The annular combustor is comprised of a prediffuser, a dump diffuser, and a liner with dilution holes. The optimizer selects a value of M3' (the Mach number after the dump diffuser) and seeks to maximize the ratio of Po4/Po3, thereby minimizing stagnation pressure loss across the combustor. To analyze each combustor design as fmincon

iterates, the solver begins by calculating the fuel ratio f using the given To4, Cp, fuel heating value, and combustion efficiency, along with the inlet To3 provided by the compressor. Then, it assumes that the prediffuser inlet dimensions are equal to the compressor outlet dimensions before using a user-selected area ratio and mean radius ratio to calculate the prediffuser outlet dimensions and prediffuser length. Next, it uses the selected value of M3' to solve for A3', which is the annular area immediately after the dump diffuser. It subsequently uses A3 (prediffuser inlet area), M3 (from the compressor exit/prediffuser inlet), and A3' to calculate the Po loss across the diffuser, treating the prediffuser and dump diffuser as one dump diffuser together. This means that the prediffuser is technically arbitrary as pertaining to Po loss, so all values associated with the prediffuser (expansion angle, area ratio, etc) were chosen from typical ranges for the sake of providing quantities. The solver also assumes that the diffuser is adiabatic such that To3' = To3. Next, it calculates static properties in the flame tube using M3', Po3', and To3', after which it estimates the flame tube length using rho3', mdot, A3', and the residence time. It then calculates the combustor hot losses using To3, To4, A3, A3', Po3, and M3, before combining it with the cold losses previously calculated to obtain a final value of Po4.

Though this is the objective of the optimizer, there are more geometric quantities that need to be calculated. First, the code calculates the liner effective hole area (ie CdA) using the prescribed dPo/Po3 ratio. Then, it calculates the liner area and liner depth using a prescribed ratio of annulus area to liner area that the user selects. Since these areas are non-trivial, brief analysis is performed to justify the ratio. Using the prescribed snout mass fraction ratio, static pressure is evaluated inside and outside the liner. Then, "stiffness" is calculated (ie, pressure delta from outside -> inside, normalized by the pressure inside). The area ratio was manually selected such that the "stiffness" was ~5% - this aims to provide sufficient margin for continuous steady operation against downstream pressure fluctuations. Next, the diffuser length is calculated using approximate ratios taken from the notes to obtain dump gap and dome radius. Total combustor length is then calculated by summing the diffuser and flame tube lengths. Finally, the inner and outer radii at station 3' are calculated using A3' and the mean radius ratio. This mean radius ratio designates the combustor mean radius relative to the compressor mean radius and was manually adjusted to give a smooth transition to the mean radius of the turbine, which follows the combustor. Once optimization is complete, the combustor passes its exit properties (To4, Po4, f) to the turbine.

DESIGN PARAMETERS FOR OPTIMIZATION – COMBUSTOR	
M3'	Mach number after dump diffuser

EQUATIONS USED – COMBUSTOR	
$$f = \frac{T_{o4} - T_{o3}}{\eta_{comb}\frac{\Delta h_R}{C_p} - T_{o4}}$$	Used to obtain fuel-air ratio from given To4
$$h_e = h_i * \left(\frac{r_{m,comp}}{r_{m,comb}}\right) * \left(\frac{A_{e,prediff}}{A_{i,prediff}}\right)$$	Used to obtain prediffuser exit height
$$\frac{A_{3'}}{A_3} = e^{\frac{\gamma_3 M_3^2}{2}\left\{\left(1-\frac{A_3}{A_{3'}}\right)^2+\left(1-\frac{A_3}{A_{3'}}\right)^6\right\}} \frac{M_3}{M_{3'}}\left\{\frac{\left(1+[(\gamma_3-1)/2]M_{3'}^2\right)}{\left(1+[(\gamma_3-1)/2]M_3^2\right)}\right\}^{\frac{\gamma_3+1}{2(\gamma_3-1)}} \quad \text{(IV.13)}$$	Used to calculate A3' from choice of M3'
$$\frac{p_{o3'}}{p_{o3}} = e^{\frac{-\gamma_3 M_3^2}{2}K_t} \quad \& \quad K_t = \left(1-\frac{A_3}{A_{3'}}\right)^2 + \left(1-\frac{A_3}{A_{3'}}\right)^6$$	Used to calculate Po3' from choice of M3' and resultant A3'
$$L_c \approx \frac{3\dot{m}_3}{\rho_{3'} A_{ref}}\tau_{res}$$	Used to estimate flame tube length
$$L_d = L_{pre} + L_{dump} = \left(\frac{h_e - h_i}{2\tan\theta}\right) + \left(d_g + r_d\right) \quad \text{(IV.14)}$$	Used to calculate length of entire diffuser
$$\frac{\Delta p_{o,h}}{q_{ref}} \cong \frac{T_{o4}}{T_{o3}} \ln \frac{T_{o4}}{T_{o3}}$$	Used to calculate hot loss PLF
$$\frac{\Delta p_o}{p_{o3}} = \frac{\Delta p_o}{q_{ref}}\left(\frac{A_3}{A_{ref}}\right)^2 \frac{(\gamma_3/2)M_3^2}{\left(1+\frac{\gamma_3-1}{2}M_3^2\right)^{\frac{\gamma_3}{\gamma_3-1}}}$$	Used to calculate actual Po loss from PLFs
$$\left(\frac{A_{Lh,eff}}{A_{ref}}\right)^2 = \frac{1}{\frac{\Delta p_{o3,4}}{q_{ref}} - \frac{\Delta p_{o,diff}}{q_{ref}}} = \frac{q_{ref}}{\Delta p_{o,L}}$$	Used to calculate effective liner hole area from prescribed pressure drop
$$D_L = \frac{A_L}{2\pi r_m}$$	Used to obtain liner depth
$$A_{3'} = \pi\left(r_{3',\max}^2 - r_{3',\min}^2\right) = 2\pi r_{3',m} h_{3'}$$	Used to obtain inner and outer radii at diffuser exit plane

CONSTRAINTS IMPOSED - COMBUSTOR	
$\eta_{comb} = 0.99$	Combustion efficiency
$\dot{m}_{sn} = 0.65\dot{m}$	Snout mass flow ratio
$\tau_{res} = 0.021\ sec$	Required residence time
$\Delta p_{o,L}/p_{o3} = 0.041$	Prescribed liner stagnation pressure loss
$T_{o4} = 1680\ K$	Required To4 from heat addition

Turbine (component level)

A single-stage turbine with an outlet guide vane was used to meet the engine design requirements. The overall turbine is provided with the outlet conditions of the combustor, the work requirement prescribed by the compressor, the shaft speed of the compressor, and the flow properties at the given cruise conditions by the engine. The overall turbine prescribes a work ratio to each stage based on an initial ratio. These ratios linearly decrease and multiply together to get a product of one which represents 100% of the work that needs to be done. It then passes these conditions to the first stage of the turbine (in this case the only stage). Within this first stage, a3 (first stage exit swirl angle), Reon (Reynold's number at nozzle throat), Reor (Reynold's number at rotor throat), cz (axial flow velocity), and rh (blade hub radius that is kept constant across the turbine) are design variables that the optimizer chooses values for based on given upper and lower bounds. M2, the Mach number exiting the nozzle is set to 1, as this stage's nozzle is assumed to be choked. The optimizer works towards maximizing stage efficiency while meeting the compressor's work requirement.

Next, using cz, a1 (which is assumed to be 0 degrees entering the first stage), a3, To1, Po1, M2, Cp, gamma, R, mdot, rh, and N, velocity triangle analysis was performed to calculate the total velocity, swirl velocity, and swirl angle at each station of the turbine in the casing reference frame. Then, the rh value decided by the optimizer is used to calculate the tip and mean radii for nozzle blades as well as the pitchline blade velocity. Next, this pitchline blade velocity is used to convert the previously found total velocity, swirl velocity, and swirl angle at each station to the rotor reference frame. These properties are used to calculate the stage loading coefficient, flow coefficient, and degree of reaction of the stage. Then, Zwefiel solidity relations and the given Zwefiel loading parameter are used to calculate the axial solidities and regular solidities for the nozzle and rotor blades.

The axial and regular solidities of the nozzle blades are then used, along with rm, Reon, givens, R, Cp, To1, Po1, gamma, M2, a1, a2, ctheta2, cz, and hn to perform an iterative loss calculation that found nozzle blade chord, nozzle blade spacing, nozzle energy loss coefficient, and updated the value of Po2 using a pressure loss formula. This iterative solution yielded results for the nozzle blade aspect ratio, nozzle blade count, a final nozzle loss coefficient value, and a final Po2 value.

Next, using cz, rh, mdot, To2, Po2, M2, gamma, and R, the tip and mean radii for the rotor blades are calculated. Then an iterative solution that utilized inlet conditions, stage loading coefficient, rotor axial and regular solidities, rotor geometry (rmr and hr), and velocities (c2, w2, w3, c3), was used to update the values for the rotor energy loss coefficient and the pressures for the relative frames. This yielded results for rotor blade aspect ratio, stage total pressure ratio, stagnation temperatures at the rotor's inlet and

outlet, stage exit density, a final rotor energy loss coefficient value, relative Mach number at the rotor inlet, and rotor blade chord.

From all the previous results, stage efficiency, stagnation pressure at the stage exit, stage polytropic efficiency, and work done by the stage are found. In addition, using rtr, rh, N, cz, sigmar, br, Cp, To1, To3, P1, P2, and required blade taper ratio and max thickness, rotor blade stress calculations were performed. These provided the results for AN^2, centrifugal stress, and bending stress.

The same general process was used in the calculations for values of the remaining stages. However, for the remaining stages, cz and rh chosen by the first stage's optimizer were passed to the remaining stages to keep those properties constant across the turbine. Another difference was that the remaining stages were not assumed to have choked nozzles. As a result, M2, the exit Mach number of each stage's nozzle, was a design variable that had its value chosen by the optimizer. In the process of developing our preliminary engine design, it was found that only one stage was needed to meet the design requirements. This meant that the remaining stages and associated analysis were not needed.

The single turbine stage is followed by an outlet guide vane (OGV) that is intended to enforce the zero-exit swirl entering the nozzle condition. This is achieved by modeling the OGV as a diffuser. The optimizer aimed to enforce the exit swirl angle, a3, as 0 degrees, and to minimize pressure loss by using solidity as a design variable. In addition, it used M2, the exit Mach number, as a design variable to avoid making a choked nozzle assumption. It receives the outlet conditions of the turbine stage and then follows the same analysis process as the compressor OGV to achieve a design that meets its constraints.

DESIGN PARAMETERS FOR OPTIMIZATION - TURBINE	
a3	Rotor exit swirl angle in casing reference frame
Reon	Reynold's number at nozzle throat
Reor	Reynold's number at rotor throat
cz	Axial flow velocity
rh	Blade hub radius (constant across turbine)
M2	Mach number exiting nozzle (only for turbine stages after first
$\boldsymbol{\sigma_{OGV}}$	Solidity of outlet guide vane blade row

EQUATIONS USED - TURBINE	
$\frac{p_{o1}}{p_{o3}} = \left[1 + \frac{\gamma - 1}{\eta_{st}} \underbrace{\frac{U^2}{\gamma R T_{o1}}}_{M_b^2} \underbrace{\frac{\Delta c_{\theta_{2,3}}}{U}}_{\psi}\right]^{\gamma/(1-\gamma)}$ (II.39)	Used to solve for stage efficiency

$$\eta_p = \frac{\ln(T_{o1}/T_{03})}{\ln\left(1+\frac{1}{\eta_{st}}(T_{o1}/T_{03}-1)\right)}$$	Used to calculate polytropic efficiency
(II.40a) $$R = \frac{1}{2}\left[1-\phi(\tan\alpha_2+\tan\beta_3)\right]$$	Used to calculate degree of reaction
$$\tan\beta_3 = \tan\alpha_3 - 1/\phi$$	Used to find b2/b3 after a2/a3 are known
$$o/s \cong \cos\alpha_2$$ (II.47a)	Used to calculate spacings
$$Re_o\ (= c_2\, o\, / \nu_{throat})$$	Used to calculate throat opening distances
$$\delta \cong m\frac{\lvert\varphi\rvert}{\sigma}; m = \frac{1}{8}$$	Used to calculate deviation at rotor exit
(II.49b) $$\delta \cong 0$$	Used to calculate deviation at nozzle exit since M2=1
(II.50) $$\sigma_z \equiv b_z / s$$	Used to calculate axial chord bz
(II.51a) $$\sigma_z\psi_z = \left(\frac{c_{\theta_1}}{c_{\theta_2}}-1\right)\sin(2\alpha_2)\left\{\frac{\gamma/2\,M_2^2}{\left(1+\frac{\gamma-1}{2}M_2^2\right)^{\gamma/(\gamma-1)}-1}\right\}$$	Used to calculate axial solidities
$$\sigma = \sigma_z/\cos\xi$$ (II.52)	Used to obtain non-axial solidities
(II.53a) $$\xi \approx \alpha_{mean} = \tan^{-1}\left(c_{\theta mean}/c_z\right)$$	Used to obtain eta angle
$$c_{\theta_{mean}} = \frac{c_{\theta_1}+c_{\theta_2}}{2}$$ (II.53b)	Used to obtain cthetamean
$$\zeta = \left(\zeta^* C_j - 1\right)\left(\frac{10^5}{\mathrm{Re}_e}\right)^{1/4}$$	Used to obtain energy loss coefficients
$$\zeta^* = 1.04 + 0.06\left(\frac{\alpha_1+\alpha_2}{100}\right)^2$$	Used to obtain zeta* values
$$C_{nozzle} = 0.993 + 0.021(b_z/h)$$	Used to obtain C value for nozzle
$$C_{rotor} = 0.975 + 0.075(b_z/h)$$	Used to obtain C value for rotor
$$\mathrm{Re}_e = \frac{\rho_2 c_2 D_h}{\mu_2}$$	Used to obtain Reynold's numbers for energy loss calcs

$$D_h = \frac{2sh\cos\alpha_2}{s\cos\alpha_2 + h}$$	Used to obtain hydraulic diameter for Reynold's calcs
$$\frac{p_{o1} - p_{o2}}{p_{o1}} = 1 - \left[\frac{1 - \frac{c_2^2}{2c_pT_{o1}}\frac{1}{1-\zeta}}{1 - \frac{c_2^2}{2c_pT_{o1}}}\right]^{\gamma/\gamma-1}$$ (II.56)	Used to obtain Po losses across turbine cascade
$$\psi = \frac{\Delta h_0}{U^2} = \frac{\Delta c_{\theta 2,3}}{U}$$	Used to obtain loading coefficient
$$\frac{c_z}{U} \equiv \phi$$ (II.21)	Used to obtain flow coefficient
$$\frac{\dot{W}}{\dot{m}} = \eta_{tr} U \Delta c_{\theta 2,3}$$	Used to link work output and U, cthetas
$$M = \frac{u}{\sqrt{\gamma RT}}$$	Used to obtain Mach numbers, abs and rel
$$\dot{m} = \rho c_z \pi\left(r_t^2 - r_h^2\right)$$	Used to obtain blade radii
$$r_m^2 = \sqrt{\frac{r_t^2 + r_h^2}{2}}$$	Used to obtain pitchline radius
$$U = \frac{\pi N r_m}{30}$$	Used to obtain radius from U
$$\chi_3 = \beta_3 - \delta_r$$	Used to obtain chi3
$$\chi_2 = \alpha_2 + \delta_n$$	Used to obtain chi2

CONSTRAINTS IMPOSED - TURBINE	
$\eta_{st} = 0.995$	Shaft efficiency is 99.5%
$0.05\ m \leq rh \leq 0.15\ m$	Hub radius kept constant across turbine in this range
$1e5 \leq Re_o \leq 5e5$	Throat Reynold's numbers for turbine
$150\ \frac{m}{s} \leq c_z \leq 200\ \frac{m}{s}$	Axial velocity kept constant across turbine and OGV
$-45° \leq \alpha \leq 45°$	Exit swirl from turbine stages
$\alpha_{out} = 0°$	Exit swirl from OGV
$M_2 = 1$	Choked nozzle for first turbine stage (in this case only stage)
$\dot{W_{req}} - \dot{W_{out}} = 0$	Ensures that work done by each turbine stage matches its prescribed work required
$0.1 \leq M_2 \leq 1$	Nozzle exit Mach number for remaining turbine stages and OGV
$t_{nozz} = 0.2 \cdot b$	Maximum thickness for all stages/OGV – sitting at upper end of range was most favorable for blade stress
$R_{taper,\,nozz} = 0.5$	Blade taper ratio for nozzle blade rows (all stages)
$\lvert\psi_Z\rvert = 0.8$	Zweifel loading parameter for nozzle blade rows (all stages)
$0.1 \leq \sigma \leq 2.0$	Bounds for realistic solidity in OGV

Nozzle (component level)

A converging-only nozzle was used to meet the engine's design requirements. No optimizer was used for the nozzle as it just receives given flow conditions, turbine OGV exit conditions, and design study-provided nozzle conditions to output needed parameters. First, it calculates the pressure at the nozzle exit, static temperature at the nozzle exit (where the given nozzle adiabatic efficiency is applied), and velocity at the nozzle exit. Then the choked assumption is applied, and the choked throat area equation is applied to find the area of the throat. Since this is a converging-only choked nozzle, the throat area is equal to the exit area. To validate that this was the case, the throat/exit area was solved again using the mass flow parameter equation. As expected, both methods yielded the same result for the throat/exit area. In addition, the freestream velocity and exit Mach were calculated. The given adiabatic efficiency meant that the nozzle wasn't perfectly choked, so the exit Mach was slightly under 1. Finally, thrust was calculated using the previously calculated values.

EQUATIONS USED - NOZZLE	
$P_e = P_{o5}\left(\frac{2}{\gamma_n + 1}\right)^{\frac{\gamma_n}{\gamma_n - 1}}$	Used to solve for pressure at nozzle exit
$T_e = T_{05}\left(1 - \eta_n\left(1 - \frac{P_e}{P_{o5}}\right)^{\frac{\gamma_n - 1}{\gamma_n}}\right)$	Used to calculate static temperature at nozzle exit
$u_e = \sqrt{2c_{p,n}(T_{o5} - T_e)}$	Used to calculate velocity at nozzle exit
$u = M_{inf}\sqrt{\gamma_d R_d T_a}$	Used to calculate freestream velocity
$ST = \frac{\tau}{\dot{m}_a} = \left[(1+f)u_e - u\right] + \frac{(p_e - p_a)A_e}{\dot{m}_a}$	Used to calculate specific thrust and thrust
$TSFC = \frac{f}{ST}$	Used to calculate specific fuel consumption

CONSTRAINTS IMPOSED - NOZZLE	
$\eta_n = 0.995$	Nozzle adiabatic efficiency of 99.5%
$\gamma = 1.35$	Nozzle flow specific heat ratio
$A_e = A_{th}$	Fixed area converging nozzle used

Diffuser (component-level)

Since the first stage of the compressor and IGV essentially pick everything that dictates the structure of the diffuser, its analysis is fairly straightforward, and no optimizer is necessary. The code begins by assuming that the diffuser exit area is the annular area of the inlet guide vane. It then employs a non-isentropic, adiabatic area-Mach-number

relation along with the exit area, exit Mach number (as chosen by the compressor first stage), and freestream Mach number, which yields the inlet area and diameter. Po2 and To2 were already calculated by the first stage of the compressor and IGV using the provided recovery factor and the adiabatic assumption. Calculation of cz at the diffuser exit is carried out using isentropic relations and the diffuser exit Mach number.

EQUATIONS USED - DIFFUSER	
$\mathrm{A}_1 = A_2 * r_d * \left(\frac{M_1}{M_2}\right) * \left(\frac{1+\frac{\gamma-1}{2}M_1^2}{1+\frac{\gamma-1}{2}M_2^2}\right)^{\frac{\gamma+1}{2(\gamma-1)}}$	Used to calculate diffuser inlet area
$\mathrm{P}_{o2} = \mathrm{P}_{o1} * R_d$	Used to calculate Po at diffuser exit

CONSTRAINTS IMPOSED - DIFFUSER	
$r_d = 0.985$	Stagnation pressure recovery factor
$M_2 \leq 0.5$	Diffuser exit Mach number (technically chosen by compressor)

Off-Design Performance

Following the successful optimization of an entire engine, its off-design performance was analyzed at the given flight conditions across the required range of To4 values, assuming double-choked operation. First, since ambient conditions and freestream Mach number change, new stagnation properties at stations 1 and 2 (assuming the diffuser recovery factor remained the same, and the diffuser was still adiabatic) and the new freestream velocity were calculated. Next, assuming turbine temperature ratio, f, and shaft efficiency remained roughly the same, off-design To3 and To5 were calculated for each To4 value using both on and off design To4 and To2 as well as the on-design To3. Then, off-design compressor pressure ratio was calculated, assuming that polytropic efficiency also remained the same. From there, off-design mass flow was calculated by obtaining the corrected mass flow first via on and off-design throttle parameters and compressor pressure ratios, then uncorrecting the mass flow. Off-design RPM was calculated using the on-design corrected RPM and both on and off-design throttle parameters, and the true f was calculated using the off-design To3 and To4. Off-design turbine pressure ratio was calculated using off-design To5 and To4, assuming the polytropic efficiency of the turbine did not substantially change and the burner pressure ratio remained constant. Note that this yielded a constant turbine pressure ratio equal to the on-design ratio, which checks out given our assumption that the turbine temperature ratio remained constant. Next, diffuser inlet and exit Mach numbers M1 and M2 were calculated using the compressible mass flow equation, knowing that the areas remain the same as on-design and using the new stagnation properties and mass flow rate. Lastly, using the same methods as

described in the nozzle section, outlet static properties, exhaust velocity, thrust, ST, and TSFC were calculated using the turbine exit stagnation properties and on-design geometry.

EQUATIONS USED – OFF-DESIGN	
$\left(T_{o3}/T_{o2}\right)_{O-D} \cong 1+\left\{\left(T_{o3}/T_{o2}\right)_{D}-1\right\}\frac{\left(T_{o4}/T_{o2}\right)_{O-D}}{\left(T_{o4}/T_{o2}\right)_{D}}$	Used to obtain off-design To3
$Pr_{c,O-D} \cong \left\{\left(T_{o3}/T_{o2}\right)_{O-D}\right\}^{\frac{\gamma_{comp}\,\eta_{pc}}{\gamma_{comp}-1}}$	Used to obtain off-design compressor Pr
$f_{O-D} \cong \frac{1-T_{o3,O-D}/T_{o4,O-D}}{\eta_b\,\Delta h_r/c_{p_b}T_{o4,O-D}-1}$	Used to obtain off-design f
$\dot{m}_{c2,O-D} = \dot{m}_{c2,D}\frac{Pr_{comp,O-D}}{Pr_{comp,D}}\frac{\sqrt{\left(T_{o4}/T_{o2}\right)_{D}}}{\sqrt{\left(T_{o4}/T_{o2}\right)_{O-D}}}$	Used to obtain off-design corrected mdot
$\frac{N_{c2,O-D}}{N_{c2,D}} \approx \frac{\sqrt{\left(T_{04}/T_{02}\right)_{O-D}}}{\sqrt{\left(T_{04}/T_{02}\right)_{D}}}$	Used to obtain off-design corrected RPM
$\dot{m}_{2,D} = \dot{m}_{c2,D}\frac{p_{o2}/p_{ref}}{\sqrt{T_{o2}/T_{ref}}}$	Used to obtain actual mdot from corrected
$N_{OD} = N_{C,OD} * \sqrt{\frac{T}{T_{ref}}}$	Used to obtain actual RPM from corrected
$\frac{p_{o4}}{p_{o5}} = \left(\frac{T_{o4}}{T_{o5}}\right)^{\gamma_{turb}/\left[\left(\gamma_{turb}-1\right)\eta_{pt}\right]}$	Used to obtain turbine pressure ratio

RESULTS

General Engine Values

RPM	$\dot{W}_{comp}$ (MW)	$\dot{W}_{turb}$ (MW)	FAR	ST (m/s)	SFC (s/m)	Thrust (kN)
27992	1.556	1.564	0.03511	829.7	4.23e-5	4.165

Diffuser/Inlet Values

D_i (m)	$A_{e,diff}$ (m^2)	M_1	P_{o2} (kPa)	M_2	cz_2 (m/s)
0.2001	0.0412	0.8	67.72	0.5	163.9

Compressor IGV

$cz_{2.1}$ (m/s)	rh_2 (m)	rt_2 (m)	rm_2 (m)	N_{blades}	χ_{out} (°)	a_2 (°)	σ	h/b	$P_{o2.1}$ (kPa)
163.9	0.0499	0.1249	0.0951	41	28.43	25	0.911	5.65	67.19

Compressor Overall

N_{stages}	cz (m/s)	P_{o3} (kPa)	T_{o3} (K)	η	η_{poly}
7	163.91	738.12	280.872	0.8910	0.9207

Compressor Stages

Stage	rh (m)	rt (m)	rm (m)	ϕ	ψ	Pr	η	°R	M1rel	a3 (°)
1	0.045	0.125	0.094	0.596	0.522	1.53	0.921	0.47	0.79	27.5
2	0.075	0.125	0.103	0.543	0.462	1.49	0.923	0.50	0.78	30
3	0.090	0.125	0.109	0.514	0.435	1.45	0.923	0.50	0.75	32.5
4	0.099	0.125	0.113	0.496	0.419	1.41	0.923	0.49	0.71	35

5	0.105	0.125	0.116	0.484	0.406	1.37	0.923	0.47	0.67	37.5
6	0.110	0.125	0.117	0.476	0.392	1.33	0.924	0.45	0.62	40
7	0.112	0.125	0.119	0.470	0.373	1.29	0.925	0.44	0.58	42.5

Stage	N_{blades}	χ_{out} (°)	Df	σ	Re_b	h/b	P_{oe} (kPa)	AN^2 (m^2RPM^2)	σ_c/ρ (m^2/s^2)	σ_{bend} (Pa)
1.r	11	-25.2	0.535	1.36	7.91e5	1.1	104.5	6.68e7	5.16e4	2.43e4
1.s	13	18.6	0.533	1.19	7.30e5	1.1	102.8	-	-	-
2.r	17	-30.8	0.537	1.19	6.45e5	1.1	155.5	4.92e7	3.83e4	6.08e4
2.s	19	22.2	0.529	1.07	6.05e5	1.1	153.2	-	-	-
3.r	27	-32.8	0.538	1.25	5.61e5	1.1	225.5	3.69e7	2.88e4	12.5e4
3.s	27	25.4	0.528	1.05	5.39e5	1.1	222.4	-	-	-
4.r	37	-33.3	0.538	1.22	4.98e5	1.1	318.3	2.93e7	2.21e4	22.8e4
4.s	37	28.6	0.527	1.05	4.96e5	1.1	314.1	-	-	-
5.r	49	-32.9	0.537	1.20	4.46e5	1.1	436.6	2.21e7	1.74e4	38.7e4
5.s	47	31.8	0.525	1.02	4.64e5	1.1	431.2	-	-	-
6.r	63	-32.2	0.533	1.19	4.03e5	1.1	581.8	1.77e7	1.39e4	61.7e4
6.s	55	35.0	0.520	0.94	4.38e5	1.1	575.0	-	-	-
7.r	77	-31.3	0.526	1.16	3.65e5	1.1	752.3	1.45e7	1.14e4	93.3e4
7.s	61	38.4	0.511	0.84	4.16e5	1.1	744.3	-	-	-

Compressor OGV

rh (m)	rt (m)	rm (m)	N_{blades}	χ_{out} (°)	a_{out}(°)	σ	Re_b	h/b	P_{oe} (kPa)
0.115	0.125	0.120	81	-13.5	0.0	1.01	2.85e5	1.1	738.12

Combustor

L_{diff} (m)	$r_{inner,3'}$ (m)	$r_{m,3'}$ (m)	$r_{outer,3'}$ (m)	$M_{3'}$	$L_{fl\ tube}$ (m)	D_L (m)	$A_{h,eff}$ (cm^2)	T_{o4} (K)	P_{o4} (kPa)	P_{o4}/P_{o3}
0.019	0.120	0.133	0.146	0.117	0.343	0.021	105	1680	658.3	0.892

Turbine Overall

N_{stages}	T_{o5} (K)	P_{o5} (kPa)	η	η_{poly}	cz (m/s)
1	1444.8	300.63	0.889	0.902	175.76

Turbine Stage

Stage	ϕ	ψ	η	°R	cz_e(m/s)
1	0.419	-1.773	0.895	0.17	175.76

Stage	rh (m)	rt (m)	rm (m)	N_{blades}	χ_{out} (°)	a_{out} (°)	σ	h/b	P_{oe} (kPa)	M_e	AN^2 (m^2RPM^2)	σ_c/ρ (m^2/s^2)	σ_{bend} (Pa)
1.n	0.130	0.155	0.143	23	76.3	76.3	1.02	0.60	624.38	1	-	-	-

1.r	0.130	0.168	0.151	23	-79.9	-8.1	1.39	0.66	302.38	0.24	5.57e7	3.59e4	12.94e4

Turbine OGV

rh (m)	rt (m)	rm (m)	N_{blades}	χ_{out} (°)	a_{out}(°)	σ	h/b	P_{oe} (kPa)	M_e
0.130	0.193	0.164	35	-0.95	0	1.06	2	300.63	*0.55*

Nozzle

A_{th}	A_e	P_e (kPa)	T_e (K)	u_e (m/s)	M_e
0.0165	0.0165	161.40	1240.4	675.89	1

Off-Design Performance

T_{o4} (K)	$\dot{m}_{air}$ (kg/s)	M1	M2	RPM	FAR	Pr_c	Pr_T	ST (m/s)	SFC (s/m)	Thrust (kN)
1550	2.44	0.285	0.216	26887	0.0325	11.32	0.466	803.0	4.04e-5	1.96
1650	2.64	0.310	0.235	27741	0.0352	12.62	0.466	851.7	4.13e-5	2.24

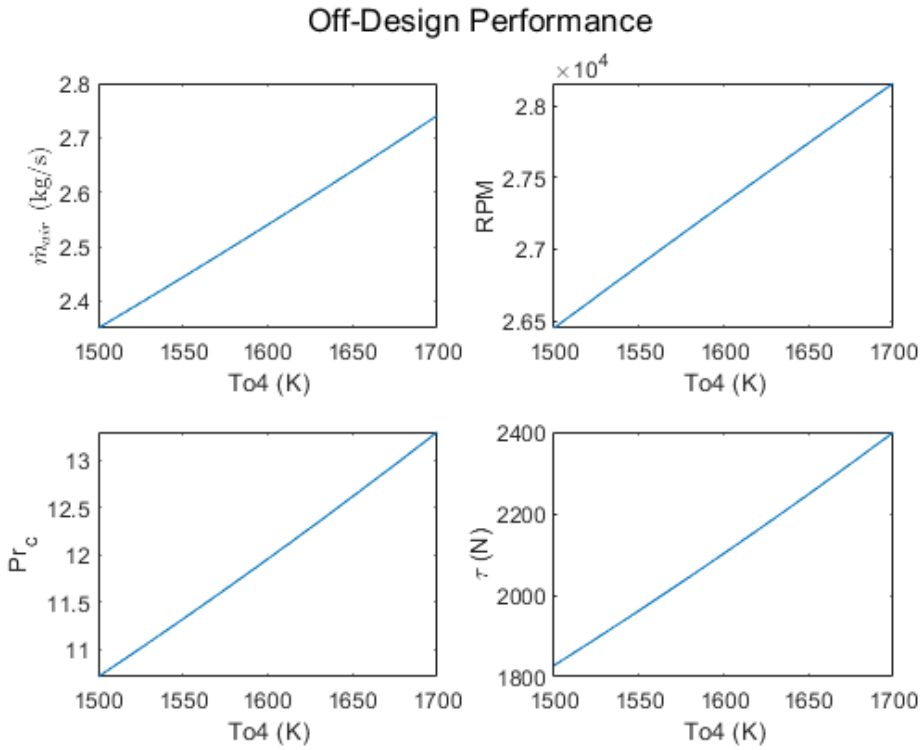

Figure 1. Off-Design Performance

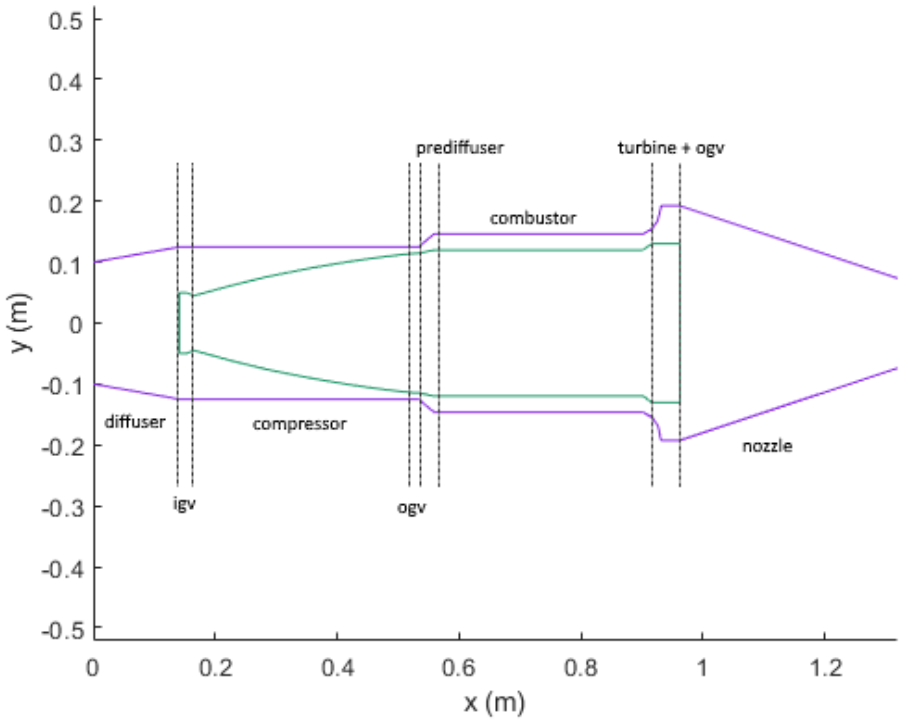

Figure 2. Engine Sketch

As shown above, the final design yielded a thrust value of 4.165 kN, which is close to the original target of 4.3 kN. Efficiencies for all components were reasonable. Diffuser and nozzle efficiencies were fixed per the prompt, the polytropic compressor and turbine efficiencies were >90%, and the stagnation pressure loss in the combustor was just over 10%, all of which are reasonable component efficiencies with no glaringly subpar designs. This means that the preliminary cycle design analysis was likely under conservative in its assumed component efficiencies.

The compressor was able to hit its target pressure ratio with seven stages. This stage count was selected to balance overall efficiency with total blade count for practical considerations. The solver selected a high RPM and a low radius, which makes sense given the relative size and mass flow of the engine. Stage loading and flow coefficients remained within reasonable ranges – stage loading decreased across the engine which makes sense given the decreasing pressure ratios, and flow coefficients increased which also makes sense given that cz remained constant while rm (and U) increased. Blade counts were not excessive, though they did increase significantly across the engine, which agrees with intuition. All constraints were met with the exception of the originally specified minimum blade Reynold's number of 5e5. The solver was unable to meet this requirement in later stages without exceeding the diffusion factor constraint or dramatically undershooting the necessary pressure ratio, so it was amended to a minimum value of 2.5e5. Blade stresses

and AN^2 values all remained within reasonable ranges. Centrifugal stresses and AN^2 decrease moving axially through compressor, which makes sense given that blades become shorter. Bending stresses increase, which also agrees with intuition given that static pressures increase and blade thicknesses decrease. The IGV and OGV lowered total efficiency beyond that of any stage due to their fixed pressure ratios, meaning a more efficient solution is likely attainable if the IGV/OGV pressure ratios were dynamically optimized and maximized.

The combustor minimized stagnation pressure loss to a reasonable value considering the amount of heat addition performed. The selected optimal value of M3' was close to 0.1, which is reasonable per typical design ranges. The length was primarily driven by the flame tube, which comprised a significant portion of the total engine length. This agrees with the sentiment that combustor length is only a weak function of engine size – the engine analyzed in HW #6 was significantly larger than this engine, yet their combustors were very close in length.

The turbine was able to meet the compressor-imposed work requirement with only one stage. The solver selected a high axial velocity and a relatively large pitchline radius, which had the effect of increasing stage loading at the expense of increased blade stresses and increased rotor pressure loss due to a higher relative Mach number. Were a near-constant outer mold line to be desired for practical considerations, multiple stages would likely be necessary to meet the work output. All constraints were met, and the final stagnation pressure ratio was slightly below 50% (primarily driven by the rotor), which is reasonable for a single stage of this size. Pressure loss across the outlet guide vane was also minimal, as the turbine exit swirl angle was less than ten degrees which is not extreme. Blade stresses were all within reasonable ranges, and bending stresses were lower than in the compressor since the less dense, hot gases yielded taller, thicker blades.

The nozzle imparted roughly equal parts pressure and momentum thrust to the engine. Since no optimization was performed here, there remains little to be done to increase total thrust besides increasing the assumed nozzle efficiency, which in turn moves it closer to an isentropic device that converts all available stagnation temperature into velocity and momentum. For plotting, a mellow convergence angle of 20° was used to give a more conservative estimate of length without increasing the likelihood of flow separation or the influence of boundary layer effects. The nozzle exit area was less than the inlet area of the diffuser, which can be rationalized via the compressible mass flow equation given that stagnation properties and Mach number were both higher at the engine exit as opposed to the inlet.

The diffuser was effectively designed entirely by the compressor first stage, which chose to maximize the diffuser exit Mach number as much as allowed by the constraints. This was optimal for compressor efficiencies and blade Reynold's numbers, though it did

have the effect of increasing the range of stagnation pressure losses incurred by the IGV, along with blade counts.

The engine performed fairly well under the off-design cruise conditions. Due to the significantly reduced mass flow, overall thrust decreased by a factor of roughly two, while specific thrust and specific fuel consumption lingered in the same range as their on-design value. Turbine pressure ratio remained constant due to assumptions made during the analysis process, while compressor pressure ratio increased. RPM generally decreased from its on-design value, though this depends on the value of To, indicating that RPM is more dependent on throttle parameter as opposed to freestream conditions. Mach number at the diffuser inlet and exit both decreased, which agrees with intuition given the significantly lowered mass flow, modified inlet stagnation properties, and fixed areas.

CONCLUSIONS

The nominal thrust produced by this engine design came close to the target thrust of 4.3 kN, though it ultimately fell short by roughly 150 N. Since all component efficiencies were optimized to be as high as possible given the provided set of constraints, it is likely that the efficiencies used during the preliminary cycle design analysis were slightly too high. That being said, many of the analysis methods did leave some fidelity to be desired, so it is possible that the target thrust is feasible. For example, the combustor diffuser was simply analyzed as a dump diffuser despite the presence of a prediffuser. Were analysis to be reperformed accounting for the decreased stagnation pressure loss due to the presence of the prediffuser slowing the flow prior to the dump, it is likely that combustor losses would decrease, in turn increasing the stagnation pressure at the nozzle exit and the thrust.

The compressor was able to obtain the given pressure ratio with a reasonable number of stages, and the single-stage turbine needed to drive it given the provided shaft efficiency was feasible and reasonably sized. To increase thrust to meet the 4.3 kN target, compressor pressure ratio could be increased and more stages added. Additionally, the heat added by the combustor was driven by the desire to avoid bleed air cooling in the turbine; with the addition of a bleed system or the selection of a slightly more robust alloy for the turbine blades, To4 could be increased slightly, which would in turn allow for higher stagnation temperature in the nozzle, a higher exhaust velocity, and increased thrust. Conversely, more heat could be added to increase stagnation temperature *after* the turbine instead (ie, an afterburner), which would increase thrust at the expense of increased TSFC.

The geometry presented by this engine appeared feasible and realistic – solidities, blade counts, and blade stresses generally fell within typical value ranges. That being said, geometric quantities such as component lengths and flow turning angles were not particularly well characterized or weighted in the optimization process. In a real vehicle, where having a longer or wider engine negatively impacts system-level performance, those considerations become more important. In addition, while geometry and stress-

characterizing values, such as AN^2, did fall in realistic ranges, in an optimization of an actual engine design, these values would have to be considered alongside information regarding available materials, manufacturing methods/capabilities, and financial costs to ensure that manufacturing the engine would be feasible. Similarly, certain optimization decisions were made in a vacuum (like choosing the hub radius of the turbine) without considering the ramifications – in this instance, having a large hub radius for a given combustor radius would require more flow turning, which would increase stagnation pressure losses and overall engine performance. However, without adequate models to characterize this and other geometric parameters, the solver was able to make these decisions in a more arbitrary fashion without consequence, which would not be the case in the real world.

The only imposed constraint the engine was unable to satisfy was the blade Reynold's number for the last four compressor stages. At this point, the blades became quite short due to the increased density, decreased flow area, and constant tip radius, which in turn decreases the chord length b (the characteristic length in the Reynold's number equation) per the minimum blade aspect ratio constraint. We attempted at length to resolve this to no avail. The solver picked all variables in the direction of satisfying this constraint – tip radius was as small as possible for the first stage, meaning that for a given annular area later on, we would have the tallest blades, the longest chord, and the highest Reynold's number. Efficiencies were optimized such that temperature stayed as low as possible in later stages for the lowest viscosity and the highest Reynold's number, and cz was maximized such that flow velocity was as high as possible across the stators (which typically had lower blade Reynold's numbers due to their lack of a rotating velocity component). Yet, we were unsuccessful. To meet this constraint in the future, hub radius could be held constant instead of tip radius. This would allow blades in later stages to be taller and have longer chord length for the same annular area, in turn driving up the Reynold's number for more favorable flow across the blade row.